2017

Point defect induced giant enhancement of flux pinning in Co-doped FeSe0.5Te0.5 superconducting single crystals

Lina Sang
University of Wollongong

Pankaj Maheswari
National Physical Laboratory India

Zhenwei Yu
University of Wollongong, zy139@uowmail.edu.au

Fei Yun
University of Wollongong, ffy486@uowmail.edu.au

Yibing Zhang
Shanghai University

See next page for additional authors

Publication Details

Sang, L., Maheswari, P., Yu, Z., Yun, F. F., Zhang, Y., Dou, S., Cai, C., Awana, V. P. S. & Wang, X. (2017). Point defect induced giant enhancement of flux pinning in Co-doped FeSe0.5Te0.5 superconducting single crystals. AIP Advances, 7 (11), 115016-1-115016-9.

Point defect induced giant enhancement of flux pinning in Co-doped FeSe0.5Te0.5 superconducting single crystals

Abstract

Point defect pinning centers are the key factors responsible for the flux pinning and critical current density in type II superconductors. The introduction of the point defects and increasing their density without any changes to the superconducting transition temperature T c , irreversibility field H irr , and upper critical field H c2, would be ideal to gain insight into the intrinsic point-defect-induced pinning mechanism. In this work, we present our investigations on the critical current density J c , H c2 , H irr , the activation energy U 0 , and the flux pinning mechanism in Fe 1-x Co x Se 0.5 Te 0.5 (x = 0, 0.03 and 0.05) single crystals. Remarkably, we observe that the J c and U 0 are significantly enhanced by up to 12 times and 4 times for the 3at.% Co-doped sample, whereas, there is little change in T c , H irr , and H c2 . Furthermore, charge-carrier mean free path fluctuation, δl pinning, is responsible for the pinning mechanism in Fe 1-x Co x Se 0.5 Te 0.5 .

Disciplines

Engineering | Physical Sciences and Mathematics

Publication Details

Sang, L., Maheswari, P., Yu, Z., Yun, F. F., Zhang, Y., Dou, S., Cai, C., Awana, V. P. S. & Wang, X. (2017). Point defect induced giant enhancement of flux pinning in Co-doped FeSe0.5Te0.5 superconducting single crystals. AIP Advances, 7 (11), 115016-1-115016-9.

Authors

Lina Sang, Pankaj Maheswari, Zhenwei Yu, Fei Yun, Yibing Zhang, Shi Xue Dou, Chuanbing Cai, V P. Awana, and Xiaolin Wang

Point defect induced giant enhancement of flux pinning in Co-doped $FeSe_{0.5}Te_{0.5}$ superconducting single crystals

Lina Sang, Pankaj Maheswari, Zhenwei Yu, Frank F. Yun, Yibing Zhang, Shixue Dou, Chuanbing Cai, V. P. S. Awana, and Xiaolin Wang

Citation: AIP Advances **7**, 115016 (2017);

View online: https://doi.org/10.1063/1.4995495

View Table of Contents: http://aip.scitation.org/toc/adv/7/11

Published by the American Institute of Physics

Point defect induced giant enhancement of flux pinning in Co-doped $FeSe_{0.5}Te_{0.5}$ superconducting single crystals

Lina Sang,[1,2] Pankaj Maheswari,[3] Zhenwei Yu,[1] Frank F. Yun,[1] Yibing Zhang,[2] Shixue Dou,[1] Chuanbing Cai,[2,a] V. P. S. Awana,[3] and Xiaolin Wang[1,4,a]
[1]*Institute for Superconducting and Electronic Materials, Faculty of Engineering, Australian Institute for Innovative Materials, University of Wollongong, NSW 2500, Australia*
[2]*Shanghai Key Laboratory of High Temperature Superconductors, Physics Department, Shanghai University, Shanghai 200444, China*
[3]*CSIR-National Physical Laboratory, Dr. K.S. Krishnan Marg, New Delhi 110012, India*
[4]*ARC Centre of Excellence in Future Low-Energy Electronics Technologies, University of Wollongong, NSW 2500, Australia*

(Received 12 July 2017; accepted 4 November 2017; published online 15 November 2017)

Point defect pinning centers are the key factors responsible for the flux pinning and critical current density in type II superconductors. The introduction of the point defects and increasing their density without any changes to the superconducting transition temperature T_c, irreversibility field H_{irr}, and upper critical field $H_{c2,}$ would be ideal to gain insight into the intrinsic point-defect-induced pinning mechanism. In this work, we present our investigations on the critical current density J_c, H_{c2}, H_{irr}, the activation energy U_0, and the flux pinning mechanism in $Fe_{1-x}Co_xSe_{0.5}Te_{0.5}$ (x = 0, 0.03 and 0.05) single crystals. Remarkably, we observe that the J_c and U_0 are significantly enhanced by up to 12 times and 4 times for the 3at.% Co-doped sample, whereas, there is little change in T_c, H_{irr}, and H_{c2}. Furthermore, charge-carrier mean free path fluctuation, δl pinning, is responsible for the pinning mechanism in $Fe_{1-x}Co_xSe_{0.5}Te_{0.5}$. https://doi.org/10.1063/1.4995495

INTRODUCTION

The potential applications of iron-based superconductors due to their relatively high superconducting critical temperature, T_c, upper critical field, H_{c2}, low anisotropy, and large current-carrying capability have become an attractive and important subject in applied superconductivity. The Fe-based superconducting systems mainly include the $REFeAsO_{1-x}F_x$ (1111-type), where RE = rare earth,[1,2] $Ba_{1-x}K_xFe_2As_2$ (122-type),[3] Li/NaFeAs (111-type),[4,5] and FeSe (11-type).[6] Nevertheless, the relatively low critical current density, J_c, is a major and challenging limiting factor for large current and high field applications. It is well known that magnetism competes against superconductivity and is detrimental to T_c. It has been shown, however, that doping with magnetic transition ions such as Mn, Cr, Co, etc. is beneficial to the appearance of superconductivity and flux pinning in various Fe-based superconductors. The superconductivity of REFeAsO (RE = La, Sm), CaFeAsF, $BaFe_2As_2$, $SrFe_2As_2$, $CaFe_2As_2$, and NaFeAs is induced by Co or Ni doping.[7–9] T_c increases with Co or Ni doping concentration in these compounds. The maximum T_c is 9 K for x = 0.06 in $SmFe_{1-x}Ni_xAsO$,[10] 20.4 K for $Ba(Fe_{0.95}\ Ni_{0.05})_2As_2$,[11] 13 K for x = 0.075 in $LaFe_{1-x}Co_xAsO$, 17.2 K for x = 0.1 in $SmFe_{1-x}Co_xAsO$,[12,13] 22 K for x = 0.1 in $CaFe_{1-x}Co_xAsF$,[14] 24 K for x = 0.0061 in $Ba(Fe_{1-x}Co_x)_2As_2$,[15] 20 K for x = 0.2 in $SrFe_{2-x}Co_xAs_2$,[16] 17 K in $CaFe_{1.94}Co_{0.06}As_2$,[17] and 21 K for x = 0.025 in $NaFe_{1-x}Co_xAs$.[9] Among them, the tetragonal Fe(Se,Te) (11-system) is an ideal and attractive platform to study superconductivity and flux pinning due to its low anisotropy, lack of poisonous elements, good stability when exposed to air, multiple band gaps, and a main Pauli

[a]Email: xiaolin@uow.edu.au; cbcai@shu.edu.cn.

paramagnetic effect in the upper critical field(s).[18–21] It is well established that $FeSe_{0.5}Te_{0.5}$ has T_c in the range of 10-15 K. We note that the Co doping changes T_c very little in $FeSe_{0.5}Te_{0.5}$ at low doping concentrations, although the T_c decreases greatly for high doping levels. There is also a lack of study on the effects of Co doping on the flux pinning and critical current density in Co-doped $FeSe_{0.5}Te_{0.5}$.

Point defects are the most important pinning centers responsible for the flux pinning and critical current density in type II superconductors. Usually, the introduction of point defects increases the irreversibility field, H_{irr}, and H_{c2}, although it reduces T_c and the effective superconducting volume. The following methods have been used to create point defects: 1) high energy ion irradiation or implantation;[22,23] 2) chemical doping;[16,24] and 3) hydrostatic pressure in granular iron pnictide superconductors.[25,26] Ideally, samples for the study of point defect induced intrinsic flux pinning should have a positive effect only on J_c due to doping, but little change in T_c, H_{irr}, or H_{c2}. In this work, we present our investigations on the J_c, H_{c2}, H_{irr}, U_0, and the pinning mechanism in $Fe_{1-x}Co_xSe_{0.5}Te_{0.5}$ (x = 0, 0.03 and 0.05) single crystals. Remarkably, we observed that the J_c is significantly enhanced by up to 12 times in the 3at.% Co-doped sample, whereas there is little change in T_c, H_{irr}, and H_{c2}. By analysing transport and magnetic data using various models, we found that the point defects induced by cobalt incorporation enhance U_0 greatly, leading to giant enhancement of J_c. Additionally, we have obtained that the dominant pinning mechanism is variation in the mean free path, δl pinning, in $Fe_{1-x}Co_xSe_{0.5}Te_{0.5}$ single crystals because of spatial fluctuations of the charge-carrier mean free path. A comprehensive vortex phase diagram is constructed and analysed for the 3at.% Co-doped sample.

EXPERIMENTAL DETAILS

Single crystals of $Fe_{1-x}Co_xSe_{0.5}Te_{0.5}$ were grown by a self-flux melt growth method. High purity (Alfa Aesar, 99.99%) Fe, Se, Te and Co powder were weighed, mixed in stoichiometric amounts, and ground thoroughly in an argon filled glove box. The mixed powder was subsequently pelletized by applying uniaxial stress of 100 kg/cm^2, and then the pellets were sealed in an evacuated ($<10^{-3}$ Torr) quartz tube. The sealed quartz tube was heated at a rate of 2 ^{o}C/min to 450 ^{o}C and kept at that temperature for 4 hours. The temperature was then increased to 1000 ^{o}C at a rate of 2 ^{o}C/min and held at 1000 ^{o}C for 24 h. Finally, the quartz ampoule was cooled down to room temperature at a rate of 10 ^{o}C/hour. The magnetotransport was measured by the standard four-probe method with a physical property measurement system (PPMS, Quantum Design) in the field range 0f 0-8 T, parallel to the c axis. Magnetic measurements at different temperatures were performed on a Quantum Design PPMS with a vibrating sample magnetometer (VSM). The J_c was calculated from the field dependent magnetization (M-H) data by the Bean model, $J_c = 20\ \Delta M/Va(1\text{-}a/3b)$, where a and b are the width and the length of the sample perpendicular to the applied field, respectively, V is the sample volume, and ΔM is the height difference in the M-H hysteresis loop.

RESULTS AND DISCUSSIONS

The temperature dependence of electrical resistivity for the un-doped, 3at.% Co-doped, and 5at.% Co-doped single crystals at different magnetic fields are shown in Fig. 1(a–c). H_{irr} and H_{c2} were calculated from the 10% and 90% values of their corresponding resistivity transitions ρ_n (where ρ_n is the normal state resistivity just before the transition), as shown in Fig. 1(d). The inset of Fig. 2(d) reveals that the T_c^{zero} is 11 K for both the un-doped and the 3at.% Co-doped samples. Furthermore, both samples show almost the same H_{irr} and H_{c2} lines (Fig. 1d). Therefore, the 3at.% Co-doped sample is indeed ideal for studying the intrinsic point defect induced pinning mechanism and determining the maximum enhancement of J_c for the Co-doped $FeSe_{0.5}Te_{0.5}$. Note that the high Co-doping level of 5at.% causes significant reduction in T_c, H_{c2}, and H_{irr} (Figs. 1d and 2d). We therefore focus our investigations on the 3% doped $FeSe_{0.5}Te_{0.5}$.

Fig. 2(a–d) shows M-H loops at 2, 4, 6, and 8 K for both un-doped and 3at.% Co-doped single crystals. As can been seen, the M-H loops of the 3at.% Co-doped sample are much wider for both

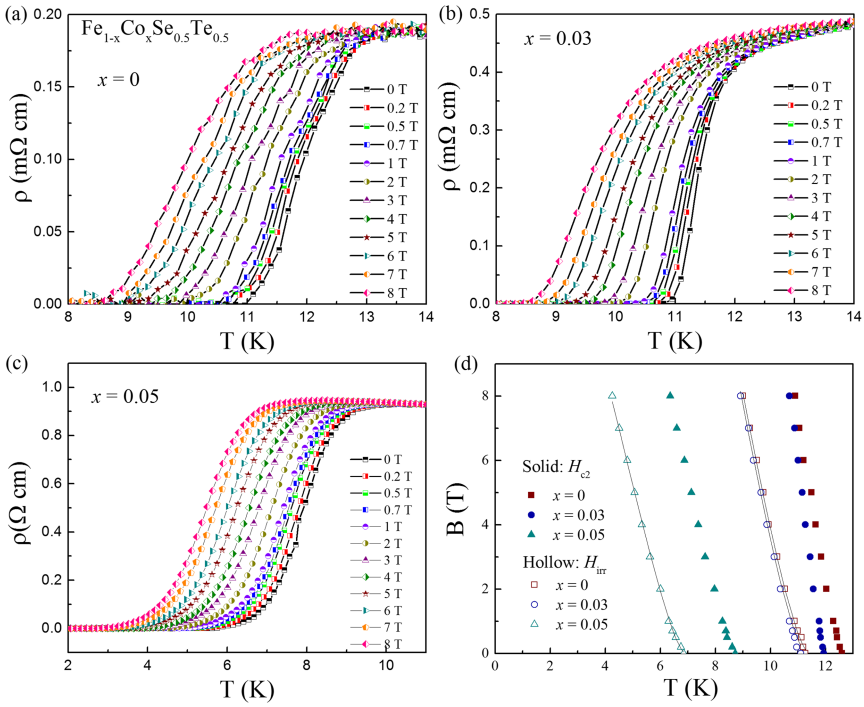

FIG. 1. (a-c) Resistivity vs. temperature in different magnetic fields, and (d) H_{c2} and H_{irr} vs. temperature for the un-doped, 3at.% Co-doped, and 5at.% Co-doped $FeSe_{0.5}Te_{0.5}$ samples.

low and high fields at different temperatures compared to the un-doped sample. It is obvious that the broadening of the loops is caused by the big enhancement of flux pinning due to the Co-doping. Fig. 3(a–d) shows J_c vs. field at different temperatures. The self-field J_c values for the un-doped

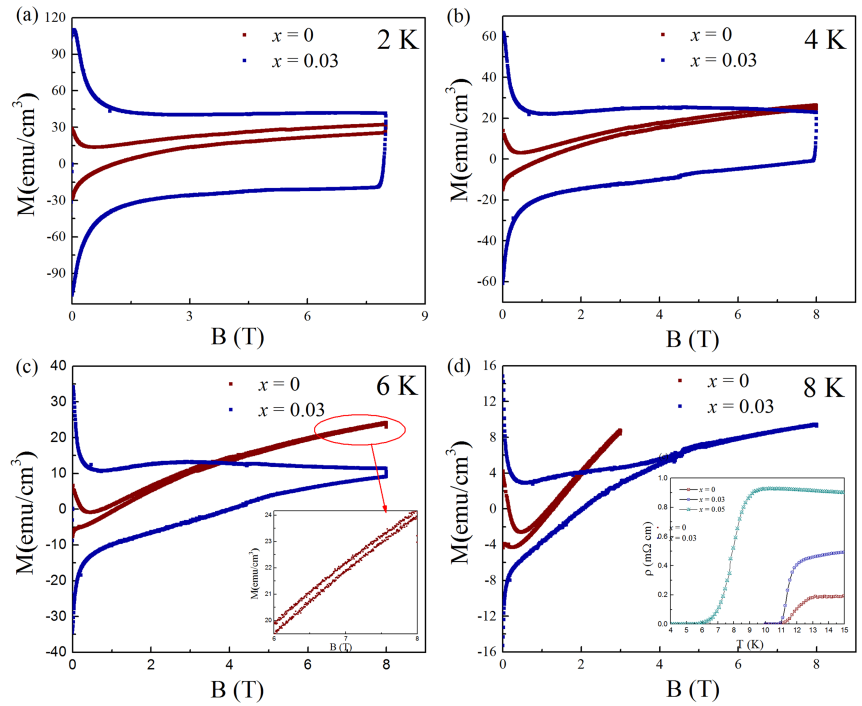

FIG. 2. (a-d) *M-H* measurements of un-doped and 3at. % Co-doped samples at 2, 4, 6, and 8 K. Inset in (c): enlargement of indicated range. Inset in (d): resistivity vs. temperature at zero field for the three samples.

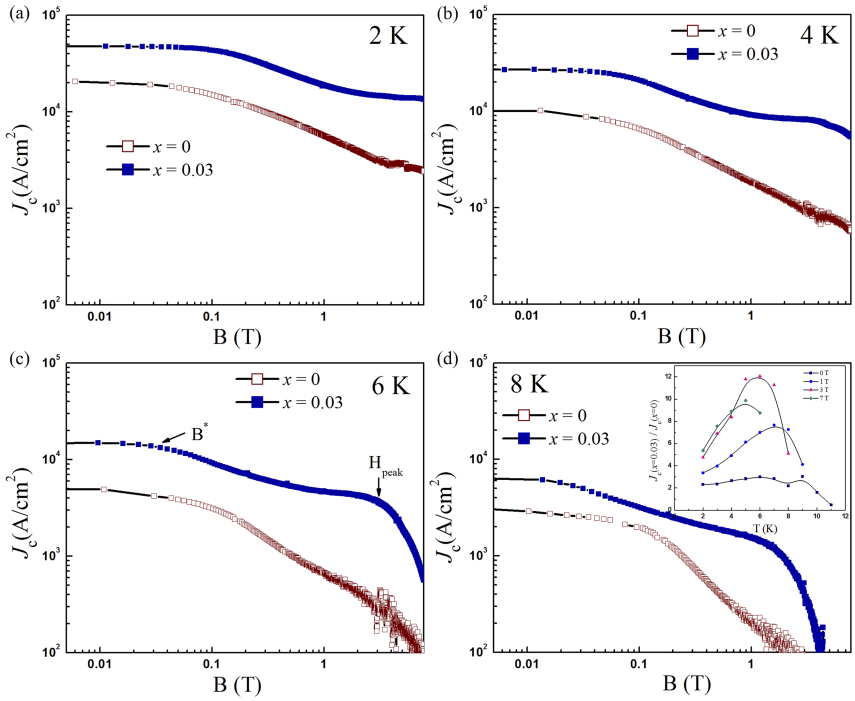

FIG. 3. (a-d) J_c vs. field at 2, 4, 6, and 8 K for un-doped and 3at.% Co-doped samples. Inset in (d): Ratio of $J_c(x{=}0.03)/J_c(x{=}0)$ vs. temperature at different fields.

sample are 2×10^4, 1×10^4, 5×10^3, and 3×10^3 A/cm^2 at 2, 4, 6, and 8 K, respectively. Remarkably, the Co-doping significantly enhances the self-field J_c to 4.7×10^4, 2.67×10^4, 1.47×10^4, and 6.7×10^3 A/cm^2 for the 3at.% Co-doped sample at 2, 4, 6, and 8 K, respectively. The enhancement of J_c is also big for high fields. Furthermore, the second magnetization peak (SMP) (in Fig. 3(c)), appears in the Co-doped sample.

To quantify the J_c enhancement, the ratio of $J_c(x{=}0.03)/J_c(x{=}0)$ vs. T at different fields was plotted as shown in the upper-right inset of Fig. 3(d). It can be seen that the ratio ranges from 2.3 at 2 K to 3 at 6 K for zero field, from 3.3 at 2 K to 7.6 at 7 K for 1 T, from 4.7 at 2 K up to 12 at 6 K for 3 T, and from 5.3 at 2 K to 9.8 at 5 K for 7 T, respectively. These results show that there is higher enhancement of J_c in the 3at.% Co-doped sample for both high field and high temperature.

Now, let us discuss the possible flux pinning mechanisms that are responsible for the significant enhancement of J_c in the 3at.% Co-doped sample. According to the Ginzburg-Landau theory, J_c obeys the power law $J_c \propto (1\text{-}T/T_c)^{\beta}$, where $\beta = 1$ or $\beta > 1.5$ corresponds to individual, non-interacting vortices or effective and strong vortex core pinning, respectively.[25–30] Fig. 4(a) shows J_c vs. $(1\text{-}T/T_c)$ at 0 and 7 T for the un-doped and 3at.% Co-doped samples using double logarithmic scaling. β is fitted to be 1.8, 1.9, and 5.6, 5 for the the un-doped and 3at. % Co-doped samples at 0 and 7 T, respectively, indicating that strong vortex core pinning is present in both the un-doped and the 3at.% Co-doped sample.

We further analyse our data using collective pinning theory. There are two main core pinning mechanisms: δT_c pinning (randomly distributed spatial variation in T_c) and δl pinning (spatial variation in the charge carrier mean free path l), which display a different behavior in J_c as a function of temperature in the single vortex pinning regime. Based on the theoretical approach proposed by Griessen et al., the J_c obeys the following laws, respectively:

$$\delta l \text{ pinning:} \quad J_c(t)/J_c(0) = (1-t^2)^{5/2}(1+t^2)^{-1/2} \tag{1}$$

$$\delta T_c \text{ pinning:} \quad J_c(t)/J_c(0) = (1-t^2)^{7/6}(1+t^2)^{-6/5} \tag{2}$$

where $t = T/T_c$[31,32]

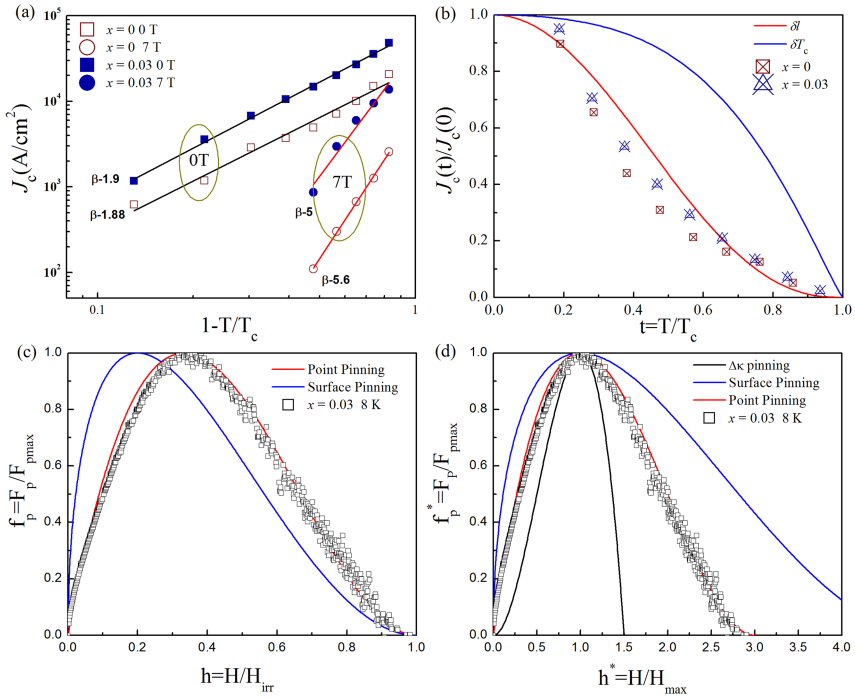

FIG. 4. (a) Logarithmic plot of J_c vs. temperature at 0 T and 7 T for the un-doped and 3at.% Co-doped samples; (b) Normalized measured J_c vs. $t = T/T_c$ at 0 T for the un-doped and 3at.% Co-doped samples, in good agreement with δl pinning. (c) Plots of the normalized pinning force ($f_p = F_p/F_{p,max}$) vs. $h = H/H_{irr}$, and (d) f_p^* vs. $h^* = H/H_{max}$ for the 3at.% Co-doped sample, in good agreement with point pinning.

Fig. 4(b) shows the normalized temperature dependence of the normalized self-field $J_c(t)$. The $J_c(t)$ values were obtained from the J_c-B curves (Fig. 3). The theoretical estimates of $J_c(t)/J_c(0)$ in the cases of δT_c pinning and δl pinning are plotted by solid curves. It can be seen that the experimental data for $J_c(t)$ are well described by the δl pinning mechanism for both the un-doped and the doped samples.

According to the Dew-Hughes model $f_p \propto h^m(1\text{-}h)^n$, different m and n fitting parameters can define the specific pinning mechanism. In this classical model, the exponents $m = 1$ and $n = 2$ represent point pinning, while $m = 1/2$ and $n = 2$ represent surface pinning, as was predicted by Kramer. The data is also scaled using $h^* = H/H_{max}$ (where H_{max} is the magnetic field when F_p reaches its maximum) instead of $h = H/H_{irr}$. The scaling of the $f^*(h)$ data can be given by the following equations, $f^*(h) = 3h^2(1\text{-}2h/3)$ (for Δk pinning), $f^*(h) = (9/4)h(1 - h/3)^2$ (for normal point pinning), and $f^*(h) = (25/16)h^{1/2}(1\text{-}h/5)^2$ (for surface pinning).[33,34] Fig. 4(c) (d) show the normalized pinning force $f_p = F_p/F_{p,max}$ vs. $h = H/H_{irr}$ or $f_p^* = F_p/F_{p,max}$ vs. $h^* = H/H_{max}$. The results show that the experimental data are all in good agreement with the point pinning mechanism for the 3at.% Co-doped sample.

As the 3% doping gives rise to giant enhancement in J_c, but causes only minor changes to T_c, H_{irr}, and H_{c2}, we believe that the Co doping must play a key role in the enhancement of the thermally activated energy, U_0. Now, we discuss the Co doping effect on U_0 based on the thermally activated flux flow (TAFF) model. The broadening of the resistivity transition within a magnetic field for superconductors is caused by the thermally induced creep of vortices.[35,36] Hence, the thermally activated energy as a function of resistivity ρ is described by the Arrhenius law, $\rho(T,B)=\rho_0\exp[-U_0/k_BT]$, where ρ_0 is a parameter, k_B Boltzmann's constant, and U_0 is the activation energy. The $\ln\rho(T, B)$ lines for various fields can be used to derive the same temperature T_{cross}, which should equal T_c, as shown in Fig. 5.

The thermal activation energy U_0 follows the power law $U_0 \propto B^{-\alpha}$ for $Fe_{1-x}Co_xSe_{0.5}Te_{0.5}$ (11-type) samples in Fig. 6, where the exponent α can be yield different values depending on the dominant pinning regime. For the un-doped, 3at.% Co-doped, and 5at.% Co-doped $FeSe_{0.5}Te_{0.5}$ samples,

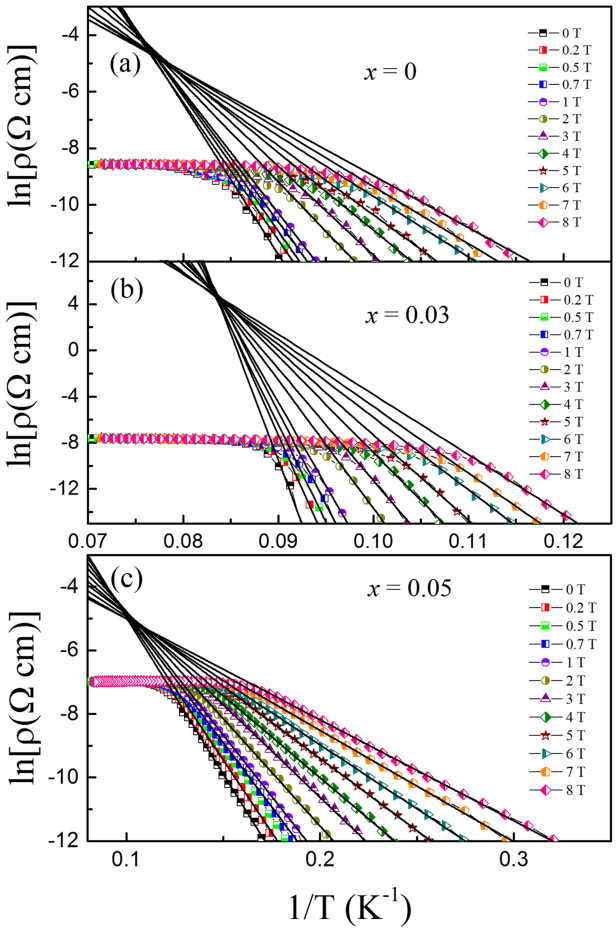

FIG. 5. Arrhenius plots of the un-doped, 3at.% Co-doped, and 5at.% Co-doped samples at different fields.

$\alpha = 0.17$, 0.14, and 0.19 when $B < 3$ T and $\alpha = 0.62$, 0.59, and 0.71 when $B > 3$ T, respectively. For $B < 3$ T, the slow decrease in U_0 indicates that single-vortex pinning dominates in this region, while for $B > 3$ T, the quick drop of $U_0(B)$ implies a crossover to collective flux creep.[31,37,38] The U_0 is 531 and 2053 K for the un-doped and 3at.% Co-doped samples at zero field, respectively. It should be noted that the U_0 values for the 3at.% Co-doped sample is four times larger than for the un-doped sample at both low and high field. As shown in Fig. 6, the pinning energy of 3at.% the Co-doped sample is two times larger than that of Bi-2212,[39] twenty times greater than that of $LaFe_{0.92}Co_{0.08}AsO$[40] with the applied field parallel to the c-axis ($H//c$), and higher than MgB_2 above 7 T.[41]

Fig. 7 shows a field-temperature phase diagram for 3at. % Co-doped sample. $B^*$and H_{peak}, as defined in Fig. 7(b) and Fig. 3(c), were obtained from $J_c(B)$ curves, while H_{irr} and H_{c2} were calculated from 10% and 90% values of their corresponding resistivity transitions in ρ_n. Based on previous studies on the SMP effect in yttrium barium copper oxide (YBCO), $FeSe_{0.5}Te_{0.5}$, and $Ba(Fe_{0.93}Co_{0.07})_2As_2$.[18,42,43] the vortex creep suddenly becomes faster, and the sample enters the plastic creep regime above H_{peak}. According to the collective pinning theory, the field dependence of J_c obeys different laws. When the field is below B^* (indicated by an arrow in Fig. 7a), the J_c is field independent, with a single-vortex pinning mechanism dominating the vortex lattice, while J_c decreases quickly above B^*, following a power law for the small-bundle-pinning regime.[44,45] Hence, the phase diagram can be clearly divided into five regions according to the strength of the applied field: (I) single vortex pinning, which is defined below B^*, (II) small bundle pinning, which governs the behaviour between B^* and H_{peak}. (III) plastic creep, which holds between H_{peak} and H_{irr}, (IV) vortex liquid, which ranges from H_{irr} to H_{c2}, and (V) the normal state, which is above H_{c2}.

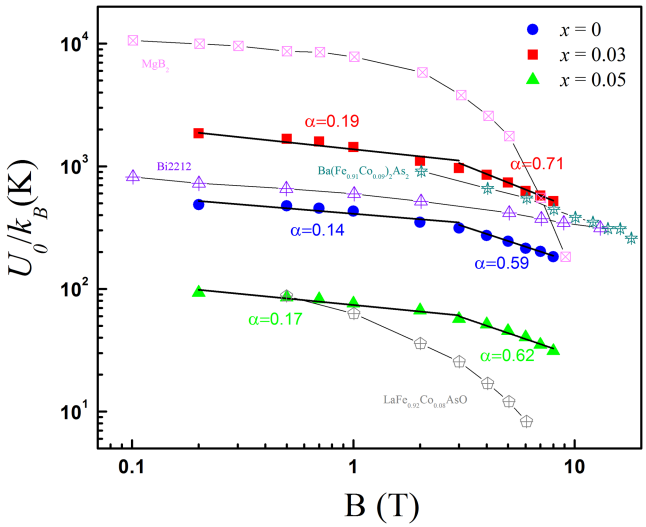

FIG. 6. Field dependence of U_0 for the un-doped, 3at.% Co-doped, and 5at.% Co-doped samples, compared with Bi-2212,[39] MgB_2,[41] Co-doped $BaFe_2As_2$(122-type),[45] and LaFeAsO(1111-type).[40]

The J_c vs. B at 6 K for both the 3at.% Co-doped and the un-doped samples has been replotted as shown in Fig. 7(a). It highlights the fact that both samples have the same H_{irr} and H_{c2}, but that the self-field J_c of the 3at.% Co-doped sample is 3 times higher than that of the un-doped sample due to Co-doping. Furthermore, the 3at.% Co-doped sample has a second magnetization peak and a high B^* compared with the un-doped sample. Based on our discussion, we conclude that it is the

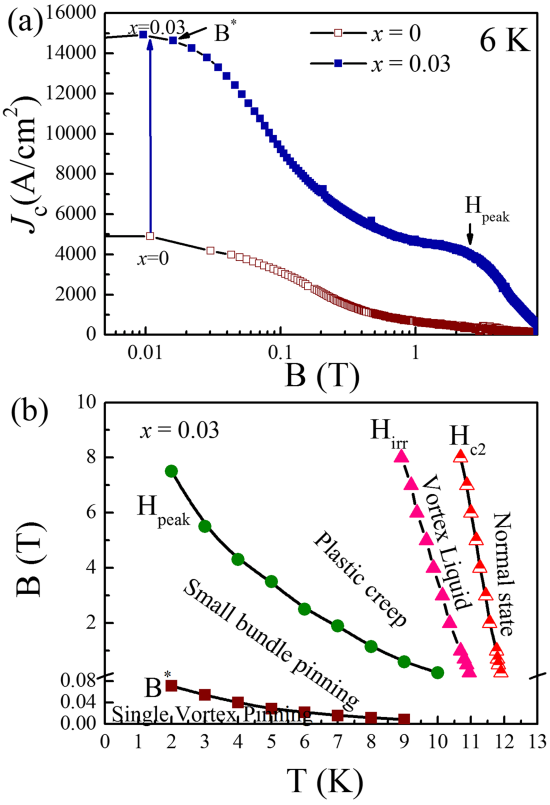

FIG. 7. (a) J_c vs. field at 6 K. (b) Phase diagram for 3at. % Co-doped sample.

enhancement of U_0 by Co-doping that is responsible for significant enhancement of the flux pining and giant enhancement of J_c in the 3at.% Co-doped $FeSe_{0.5}Te_{0.5}$ sample.

CONCLUSIONS

In summary, we have systemically studied the flux pinning mechanism for un-doped and Co-doped $FeSe_{0.5}Te_{0.5}$ samples. Remarkably, we observed that the J_c is significantly enhanced by up to 12 times in the 3at.% Co-doped sample, whereas there is little change in T_c, H_{irr}, and H_{c2}. We conclude that the point defects induced by cobalt incorporation enhance U_0 greatly leading to giant enhancement of J_c. Furthermore, the charge-carrier mean free path fluctuation, δl pinning, is responsible for the pinning mechanism in $Fe_{1-x}Co_xSe_{0.5}Te_{0.5}$.

ACKNOWLEDGMENTS

X.L.W. acknowledges support from the Australian Research Council (ARC) through an ARC Discovery Project (DP130102956) and an ARC Professorial Future Fellowship project (FT130100778). L.N.S is grateful to the China Scholarship Council (CSC) for providing her PhD scholarship. Dr. T. Silver's critical reading of this paper is greatly appreciated.

The authors declare that they have no competing interests.

[1] Y. Kamihara, T. Watanabe, M. Hirano, and H. Hosono, Journal of the American Chemical Society **130**(11), 3296 (2008).
[2] X. H. Chen, T. Wu, G. Wu, R. H. Liu, H. Chen, and D. F. Fang, Nature **453**(7196), 761 (2008).
[3] M. Rotter, M. Tegel, and D. Johrendt, Physical Review Letters **101**(10), 107006 (2008).
[4] J. H. Tapp, Z. Tang, B. Lv, K. Sasmal, B. Lorenz, P. C. W. Chu, and A. M. Guloy, Physical Review B **78**(6), 060505 (2008).
[5] D. R. Parker, M. J. Pitcher, P. J. Baker, I. Franke, T. Lancaster, S. J. Blundell, and S. J. Clarke, Chemical Communications (16), 2189 (2009).
[6] F.-C. Hsu, J.-Y. Luo, K.-W. Yeh, T.-K. Chen, T.-W. Huang, P. M. Wu, Y.-C. Lee, Y.-L. Huang, Y.-Y. Chu, and D.-C. Yan, Proceedings of the National Academy of Sciences **105**(38), 14262 (2008).
[7] M. A. Tanatar, J.-P. Reid, H. Shakeripour, X. G. Luo, N. Doiron-Leyraud, N. Ni, S. L. Bud'Ko, P. C. Canfield, R. Prozorov, and L. Taillefer, Physical Review Letters **104**(6), 067002 (2010).
[8] A. Yamamoto, J. Jaroszynski, C. Tarantini, L. Balicas, J. Jiang, A. Gurevich, D. C. Larbalestier, R. Jin, A. S. Sefat, and M. A. McGuire, Applied Physics Letters **94**(6), 062511 (2009).
[9] D. R. Parker, M. J. P. Smith, T. Lancaster, A. J. Steele, I. Franke, P. J. Baker, F. L. Pratt, M. J. Pitcher, S. J. Blundell, and S. J. Clarke, Physical Review Letters **104**(5), 057007 (2010).
[10] A. Pal, S. S. Mehdi, M. Husain, and V. P. S. Awana, Solid State Sciences **15**, 123 (2013).
[11] M. Nikolo, X. Shi, J. Jiang, J. D. Weiss, and E. E. Hellstrom, Journal of Superconductivity and Novel Magnetism **27**(9), 1983 (2014).
[12] C. Wang, Y. K. Li, Z. W. Zhu, S. Jiang, X. Lin, Y. K. Luo, S. Chi, L. J. Li, Z. Ren, and M. He, Physical Review B **79**(5), 054521 (2009).
[13] Y. Qi, Z. Gao, L. Wang, D. Wang, X. Zhang, and Y. Ma, Superconductor Science and Technology **21**(11), 115016 (2008).
[14] S. Matsuishi, Y. Inoue, T. Nomura, H. Yanagi, M. Hirano, and H. Hosono, Journal of the American Chemical Society **130**(44), 14428 (2008).
[15] J.-H. Chu, J. G. Analytis, C. Kucharczyk, and I. R. Fisher, Physical Review B **79**(1), 014506 (2009).
[16] A. Leithe-Jasper, W. Schnelle, C. Geibel, and H. Rosner, Physical Review Letters **101**(20), 207004 (2008).
[17] N. Kumar, R. Nagalakshmi, R. Kulkarni, P. L. Paulose, A. K. Nigam, S. K. Dhar, and A. Thamizhavel, Physical Review B **79**(1), 012504 (2009).
[18] P. Das, A. D. Thakur, A. K. Yadav, C. V. Tomy, M. R. Lees, G. Balakrishnan, S. Ramakrishnan, and A. K. Grover, Physical Review B **84**(21), 214526 (2011).
[19] R. Khasanov, K. Conder, E. Pomjakushina, A. Amato, C. Baines, Z. Bukowski, J. Karpinski, S. Katrych, H.-H. Klauss, and H. Luetkens, Physical Review B **78**(22), 220510 (2008).
[20] H. Kotegawa, S. Masaki, Y. Awai, H. Tou, Y. Mizuguchi, and Y. Takano, Journal of the Physical Society of Japan **77**(11), 113703 (2008).
[21] S. Khim, J. Wook Kim, E. Sang Choi, Y. Bang, M. Nohara, H. Takagi, and K. H. Kim, Physical Review B **81**(18), 184511 (2010).
[22] T. Taen, F. Ohtake, H. Akiyama, H. Inoue, Y. Sun, S. Pyon, T. Tamegai, and H. Kitamura, Physical Review B **88**(22), 224514 (2013).
[23] M. Eisterer, R. Raunicher, H. W. Weber, E. Bellingeri, M. R. Cimberle, I. Pallecchi, M. Putti, and C. Ferdeghini, Superconductor Science and Technology **24**(6), 065016 (2011).
[24] L. Sang, Y. Lu, Y. Zhang, M. Zhong, H. Zhu, Z. Liu, Y. Guo, Z. Gu, W. Qiu, and F. Fan, Superconductor Science and Technology **27**(6), 065016 (2014).
[25] B. Shabbir, X. Wang, S. Reza Ghorbani, S. Dou, C. Shekhar, and O. N. Srivastava, Scientific Reports **8213** (2015).
[26] B. Shabbir, X. Wang, S. Reza Ghorbani, A. F. Wang, S. Dou, and X. H. Chen, Scientific Reports **10606** (2015).
[27] V. Pan, Y. Cherpak, V. Komashko, S. Pozigun, C. Tretiatchenko, A. Semenov, E. Pashitskii, and A. V. Pan, Physical Review B **73**(5), 054508 (2006).

[28] M. Djupmyr, S. Soltan, H.-U. Habermeier, and J. Albrecht, Physical Review B **80**(18), 184507 (2009).
[29] J. Albrecht, M. Djupmyr, and S. Brück, Journal of Physics: Condensed Matter **19**(21), 216211 (2007).
[30] M. Djupmyr, G. Cristiani, H.-U. Habermeier, and J. Albrecht, Physical Review B **72**(22), 220507 (2005).
[31] G. Blatter, M. V. Feigel'man, V. B. Geshkenbein, A. I. Larkin, and V. M. Vinokur, Reviews of Modern Physics **66**(4), 1125 (1994).
[32] R. Griessen, W. Hai-Hu, A. J. J. Van Dalen, B. Dam, J. Rector, H. G. Schnack, S. Libbrecht, E. Osquiguil, and Y. Bruynseraede, Physical Review Letters **72**(12), 1910 (1994).
[33] D. Dew-Hughes, Philosophical Magazine **30**(2), 293 (1974).
[34] L. Klein, E. R. Yacoby, Y. Yeshurun, A. Erb, G. Müller-Vogt, V. Breit, and H. Wühl, Physical Review B **49**(6), 4403 (1994).
[35] P. K. Maheshwari, R. Jha, B. Gahtori, and V. P. S. Awana, Aip Adv. **5**(9), 097112 (2015).
[36] C. Cai, B. Holzapfel, J. Hänisch, L. Fernandez, and L. Schultz, Physical Review B **69**(10), 104531 (2004).
[37] Y. Yeshurun and A. P. Malozemoff, Physical Review Letters **60**(21), 2202 (1988).
[38] A. Leo, G. Grimaldi, A. Guarino, F. Avitabile, A. Nigro, A. Galluzzi, D. Mancusi, M. Polichetti, S. Pace, and K. Buchkov, Superconductor Science and Technology **28**(12), 125001 (2015).
[39] T. T. M. Palstra, B. Batlogg, R. B. Van Dover, L. F. Schneemeyer, and J. V. Waszczak, Physical Review B **41**(10), 6621 (1990).
[40] G. Li, G. Grissonnanche, J.-Q. Yan, R. William McCallum, T. A. Lograsso, H. D. Zhou, and L. Balicas, Physical Review B **86**(5), 054517 (2012).
[41] A. Sidorenko, V. Zdravkov, V. Ryazanov, S. Horn, S. Klimm, R. Tidecks, A. Wixforth, T. Koch, and T. Schimmel, Philosophical Magazine **85**(16), 1783 (2005).
[42] R. Prozorov, N. Ni, M. A. Tanatar, V. G. Kogan, R. T. Gordon, C. Martin, E. C. Blomberg, P. Prommapan, J. Q. Yan, and S. L. Bud'ko, Physical Review B **78**(22), 224506 (2008).
[43] Y. Abulafia, A. Shaulov, Y. Wolfus, R. Prozorov, L. Burlachkov, Y. Yeshurun, D. Majer, E. Zeldov, H. Wühl, and V. B. Geshkenbein, Physical Review Letters **77**(8), 1596 (1996).
[44] S. R. Ghorbani, X. L. Wang, S. X. Dou, S.-I. Lee, and M. S. A. Hossain, Physical Review B **78**(18), 184502 (2008).
[45] M. Nikolo, X. Shi, E. S. Choi, J. Jiang, J. D. Weiss, and E. E. Hellstrom, Journal of Superconductivity and Novel Magnetism **27**(10), 2231 (2014).